

Electronic structure and stability of $\text{Li}_{1+x}\text{Mn}_{2-x}\text{O}_4$ spinels

Helena Berg, Kenneth Göransson, Bengt Noläng and John O. Thomas*

Inorganic Chemistry, Ångström Laboratory, Uppsala University, Box 538, SE-751 21 Uppsala, Sweden. E-mail: josh.thomas@kemi.uu.se

Received 3rd November 1999, Accepted 17th March 2000

Published on the Web 4th May 2000

Trends in the electronic structure of the spinel-type manganese oxide $\text{Li}_{1+x}\text{Mn}_{2-x}\text{O}_4$, $0 \leq x \leq 1/4$, are studied using the LMTO–ASA method. The stability of the system is discussed in terms of composition (x) and the position of lithium in the structure; the influence of the latter on the total valence energy and the density-of-states (DOS) is also probed systematically. The “extra” lithium atoms are shown to prefer the octahedral 16d position for $x < 2/16$, and the octahedral 16c position for higher degrees of substitution. The open-circuit voltage reaches a maximum for $x = 1/16$.

Introduction

The electrochemical and chemical properties of LiMn_2O_4 have been studied extensively because the compound has become a widely used cathode material in rechargeable lithium-ions batteries.^{1–8} The effective capacity of batteries based on LiMn_2O_4 is known to fade significantly during the charge/discharge cycling. One of the ways to improve the cycling performance is to incorporate substituents (M) in the spinels to give the composition $\text{LiM}_x\text{Mn}_{2-x}\text{O}_4$, where M is Li, Cr, Fe, Co, Ni *etc.*^{5,6} This partial substitution of Mn considerably enhances cycling performance even for less than 10 mol% substitution;⁷ careful control of the spinel composition is thus critical to improving the capacity and cyclability of the electrode.

In the LiMn_2O_4 spinel structure (space group: $Fd3m$), lithium atoms occupy 1/8 of the tetrahedral positions (8a) and manganese atoms 1/2 of the octahedral positions (16d) in a close-packed array of oxygen atoms (32e) (Fig. 1). Lithium can be extracted from the 8a-sites to give an almost lithium-free $\lambda\text{-MnO}_2$ phase with the same space group.⁸ In transition-metal substituted spinels $\text{LiM}_x\text{Mn}_{2-x}\text{O}_4$ (M = transition metal), the substitution is a direct replacement of the manganese atoms at

their 16d positions.⁹ However, upon substitution with lithium (M = Li), the inserted lithium atoms have also been found to occupy the (16c) octahedral position, leaving the 16d position partly vacant.^{10,11} In this case, the “extra” lithium atoms are most likely to occupy the sites closest to the empty Mn sites, resulting in a local relaxation in the positions of the oxygen atoms. A possible explanation offered for the observation of lithium in two different positions is the use of different synthesis conditions. It is generally recognised that the chemical and electrochemical properties of manganese spinels are highly sensitive to the method of preparation.^{12,13} In this connection, it can be stated that the electrochemically accessible amount of Li is not increased despite the higher Li content of $\text{Li}_{1+x}\text{Mn}_{2-x}\text{O}_4$, since only the tetrahedrally coordinated lithium atoms can be extracted.¹⁴

Earlier theoretical studies of the $\text{Li}_{1+x}\text{Mn}_{2-x}\text{O}_4$ system were based on atomistic simulation methods and only took into account interatomic forces using empirical potentials describing the mean electron distribution of the electrons.^{15,16} In this work, the stability of different lithium positions in the $\text{Li}_{1+x}\text{Mn}_{2-x}\text{O}_4$ spinel phase have been investigated using *ab initio* band-structure calculations. The computational method used is the Linear Muffin Tin Orbital–Atomic Sphere Approximation (LMTO–ASA) method. The particular focus here is on chemical stability and the composition (x) dependence of the intercalation potential.

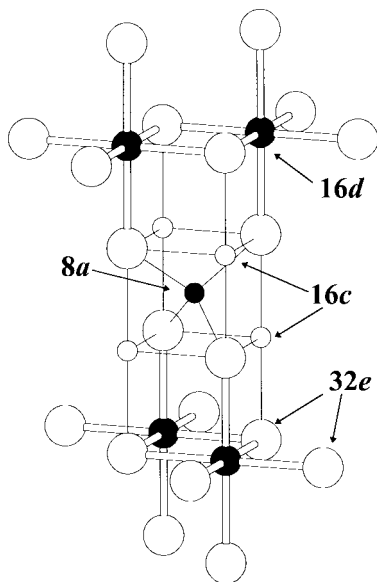
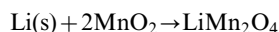


Fig. 1 A part of the cubic spinel structure (space group: $Fd3m$) showing the different atomic positions.

Calculation method

The battery potential difference is directly proportional to the difference in chemical potential for Li in the cathode and anode. In the following, a pure lithium-metal anode is assumed, and the potential of the cathode relative to the Li(s) anode is defined as the intercalation potential of lithium. This potential depends on the Li content of the cathode (x) and reflects the composition dependence of the Li chemical potential. The battery potential difference is highest at the beginning of a discharge cycle, and decreases as discharge brings more Li back into the cathode material, thus increasing the Li chemical potential. In a single-phase solid solution of lithium in a host material, the lithium content can vary and hence also the chemical potential. In a two-phase mixture, the lithium content attains the solid-solution compositional limits and the lithium chemical potential becomes constant. For such a two-phase cathode (e.g. $\text{MnO}_2 + \text{LiMn}_2\text{O}_4$), a lithium intercalation reaction can be written:



The Li intercalation potential and the battery potential difference is thus:

$$V(x) = -\frac{\Delta G}{F}$$

where ΔG is the Gibbs' free energy for the intercalation reaction, and F is the Faraday constant. In this work, ΔG ($=\Delta E + P\Delta V - T\Delta S$) is approximated by the change in internal energy (ΔE), since the calculated values are valid at 0 K when no zero-point energy is taken into account, as in these calculations. The change in internal energy is calculated from the difference in the total valence-electron energies of the compounds. The battery potential difference so obtained is the equilibrium potential difference and does not take account of resistivity effects and over-potentials caused by kinetic and diffusion limitations.

Previous attempts to derive the intercalation potential from the electronic structure for $\text{Li}_{1+x}\text{Mn}_{2-x}\text{O}_4$ spinels, *e.g.* ref. 17, involve cluster calculations. The method assumes specific valence states for the atoms, and therefore assigns charges to the clusters. The procedure has been severely criticised, *e.g.* ref. 18. In this work, the total valence-electron energies are calculated in band-structure calculations using all valence electrons and assuming full crystalline periodicity.

The computational method used for the internal-energy calculations was the LMTO-ASA method.¹⁹ The computer code used²⁰ is a local version of the code published by Skriver.²¹ Band structures and total energies were calculated for: (i) $\text{Mn}_{2-x}\text{O}_4$, (ii) $\text{LiMn}_{2-x}\text{O}_4$ (lithium atoms only at the 8a positions), (iii) $\text{Li}_x\text{Mn}_{2-x}\text{O}_4$ (lithium atoms occupying either the 16c or 16d positions), and (iv) $\text{Li}_{1+x}\text{Mn}_{2-x}\text{O}_4$ (lithium atoms occupying 8a positions and 16c or 16d positions), for $x=0, 1/16, 1/8, 3/16$ and $1/4$. All calculations assumed a perfect cubic spinel structure, *i.e.* with O at $(\frac{1}{4}, \frac{1}{4}, \frac{1}{4})$. In order to mimic the solid solution, the calculations were performed in the orthorhombic space group $Pmmm$ with $a=b=c$, thereby allowing substitution of single atoms within the unit cell. The unit cell dimensions for all structures were varied uniformly, and the theoretical sizes of the unit cells were obtained from the minimum in the total valence electron energies. Empty spheres were introduced at unoccupied octahedral and tetrahedral positions. The calculations were carried out for 84 k -points in $1/8$ of the Brillouin zone. The basis set comprised Mn s, p and d, O s and p and Li s and p functions. Inside the empty spheres, the wave functions were described by s basis functions, while the one-centre expansions were carried out upto $l=1$. The sites for substitution in the 16d case were selected as far away from one another as possible. In the 16c case, the sites were chosen such that the distance between the empty 16d sites and the "extra" lithium atoms was maximised. The distance between the empty sites and the "extra" lithium atoms is unimportant, since calculations performed with the "extra" lithium atoms as close as possible to empty 16d sites gave almost identical results.

Electronic structures

General

The total and Mn-projected density-of-states (DOS) for a lithium-free λ - MnO_2 phase at the calculated equilibrium volume is shown in Fig. 2. The band centred at around -1.35 Ry is mainly of O 2s character. In the energy interval -0.6 to -0.15 Ry, the DOS is determined by bonding interactions between O p, and Mn s, p and d orbitals. The band located around the Fermi level corresponds to non-bonding Mn d electrons. The width of this band gives evidence of some Mn-Mn interaction. Nevertheless, spin splitting and

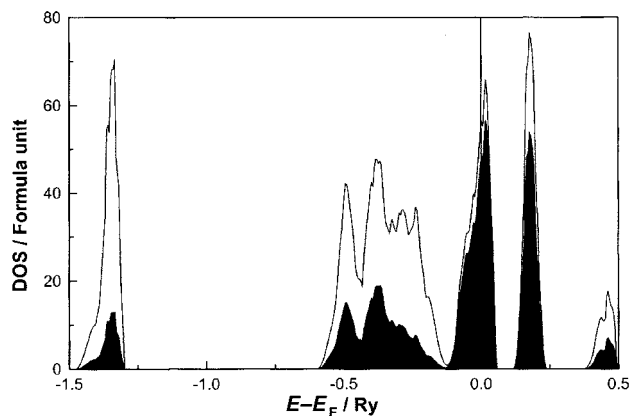


Fig. 2 Total and Mn-projected density of states (DOS) for λ - MnO_2 . The Fermi level has been shifted to zero. The DOS is given in units of number of states per formula unit and Rydberg (Ry).

the effect of on-site coulomb interactions is expected to split the Mn d states across the Fermi level.

As lithium atoms are inserted into the Mn-O framework, the lattice expands isotropically to form the LiMn_2O_4 spinel phase. The total, Li- and Mn-projected DOS's for the LiMn_2O_4 phase are shown in Fig. 3. The electrons of the inserted lithium atoms mainly enter the Mn d band and no separate Li-O bands are observed.

The lithium-site dependence

A substitution of manganese atoms by lithium atoms results in a decrease of the lattice parameter because of the smaller radius of the lithium atoms. The calculated lattice parameters, which are valid at 0 K, are less than 2% smaller than the experimental values,⁴ and have been summarised in Fig. 4. Lithium atoms at the 16c position give a larger lattice parameter than lithium atoms located at the 16d position, and follow the same trend as the experimental values. The rapid decrease in the lattice parameter for the 16d case between $x=2/16$ and $3/16$ is an effect of the constraint imposed on the lattice parameter variation, *i.e.* the a , b and c axes were not allowed to vary individually.

Comparing the DOS of $\text{Li}_{1+x}\text{Mn}_{2-x}\text{O}_4$ for $x=1/16$ (Fig. 5) with the DOS of the unsubstituted compound (Fig. 3), we can note a splitting of the oxygen 2s band due to the change in the local oxygen surroundings. Furthermore, the topmost part of the Mn-O band becomes separated from the main metal/oxygen band. In the 16c case, this effect is likely to be due to the larger cell volume. The band consists mainly of states from

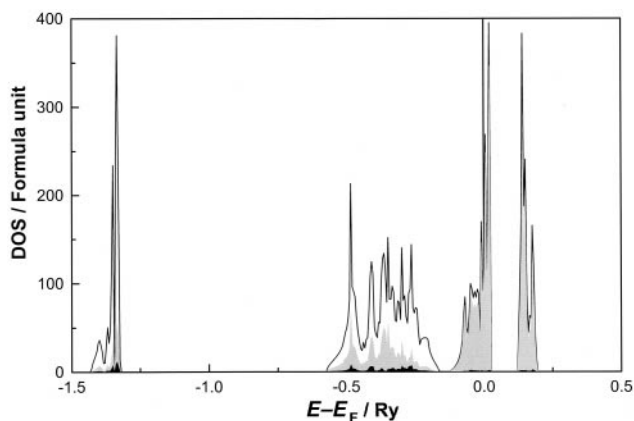


Fig. 3 The total and the Li-, and Mn-projected density of states (DOS) for LiMn_2O_4 (Li in 8a positions). The Fermi level has been shifted to zero. The DOS is given in units of number of states per formula unit and Rydberg.

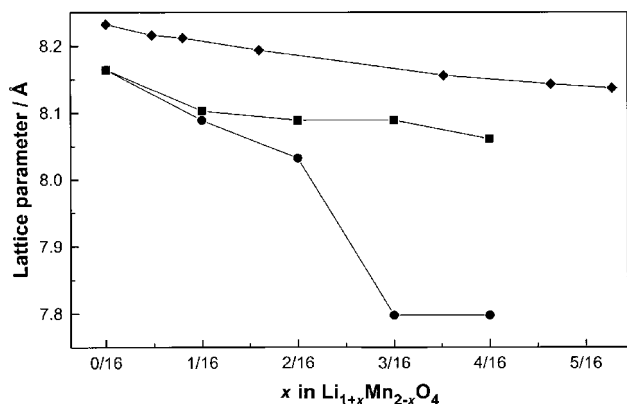


Fig. 4 The lattice parameter as a function of degree of substitution (x) in $\text{Li}_{1+x}\text{Mn}_{2-x}\text{O}_4$. ● = 16d case, ■ = 16c case, and ◆ = data from ref. 4.

oxygen atoms that surround the “extra” lithium atoms in the 16d case and oxygen atoms that surround the empty 16d position in the 16c case.

The effect of the degree of substitution (x)

The 16d case. The total DOS's for four different degrees of substitution are shown in Fig. 6. As the amount of “extra” lithium increases, the cell volume decreases, leading to a stronger Mn–O interaction and a widening of the Mn–O bonding region. The Mn non-bonding band and the Fermi level are thus shifted towards higher energies. However, the Fermi level is shifted towards lower energies with respect to the top of the Mn non-bonding band due to the reduction in the number of valence electrons per formula unit. The density of states of the two different lithium positions (8a and 16d) are shown in Fig. 7. It is clear that the highest-energy region of the oxygen s-states originates from the environment of the “extra” lithium atoms.

The 16c case. In contrast to the 16d case, the widths of the Mn–O bonding band and the Mn non-bonding band in the 16c case remain almost unchanged because of the considerably smaller decrease in volume (Fig. 8). As in the 16d case, the Fermi level is shifted towards lower energies due to the lower number of valence electrons. The topmost O s bands are, in this case, formed by the oxygen atoms around lithium atoms at 8a positions. The “extra” lithium atoms interact with oxygen atoms in the lower part of the O s band and at the bottom of the

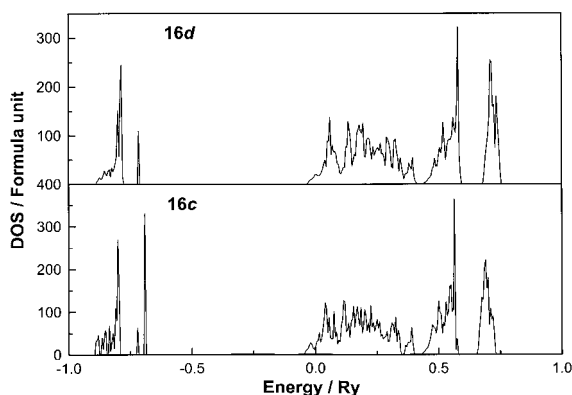


Fig. 5 Total density of states (DOS) for $\text{Li}_{1+x}\text{Mn}_{2-x}\text{O}_4$ for the 16d and 16c cases ($x=1/16$). The DOS is given in units of number of states per formula unit and Rydberg.

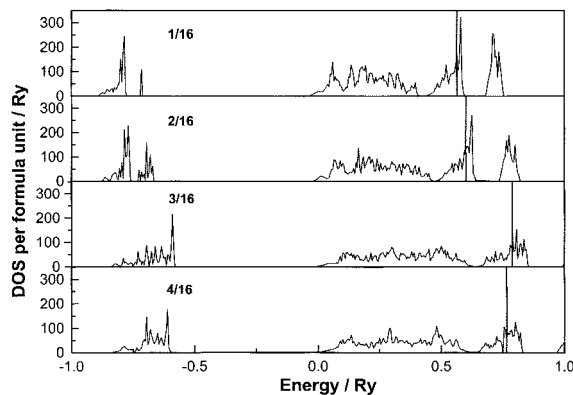
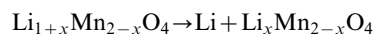


Fig. 6 Total density of states (DOS) for $\text{Li}_{1+x}\text{Mn}_{2-x}\text{O}_4$ for the 16d case. The DOS is given in units of number of states per formula unit and Rydberg.

Mn–O bonding band (Fig. 9). As the amount of “extra” lithium increases, the Li–Mn–O interactions extend to higher energies and, at higher degrees of substitution, the lithium atoms also interact with the non-bonding Mn d band.

Phase stability

The stability of the various compositions and lithium positions is summarised in Fig. 10 which gives the free energy change for the reaction:



as calculated from the total valence electron energies of the participating compounds. The 16d position is more stable than the 16c position for $x < 2/16$ while, at higher degrees of substitution, the 16c position is the most stable. It can be noted that, for low substitutions, the 16d position stabilises the structure, leading to an increase in the open-circuit voltage. Above $x=1/16$, a mixture of 16d and 16c position substitution gives a lower energy than substitution at only one of the site types; the simultaneous substitution of both site types can thus be expected. This can explain the diversity in the experimental results. The 16d position was reported as the most stable in the work of Amundsen *et al.*,²² while 16c position occupation was observed in refinements of neutron powder diffraction data.^{10,11} The preference for the 16c site was later confirmed by NMR.²³ In addition, it has been claimed that the synthesis conditions play an important rôle for the final spinel

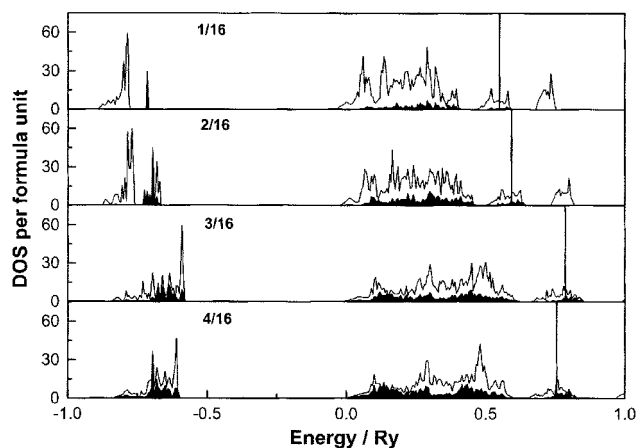


Fig. 7 The density of states (DOS) for the two types of lithium in $\text{Li}_{1+x}\text{Mn}_{2-x}\text{O}_4$ for the 16d case. The DOS is given in units of number of states per formula unit and Rydberg. The black areas are the DOS for the “extra” lithium at 16d positions; the white areas are for the lithium at 8a positions.

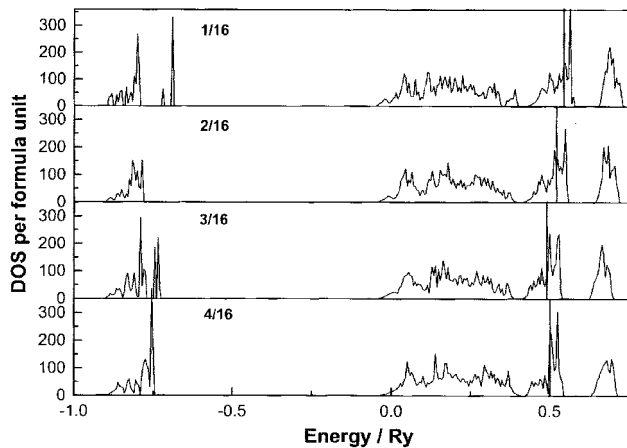


Fig. 8 Total density of states (DOS) for $\text{Li}_{1+x}\text{Mn}_{2-x}\text{O}_4$ for the 16c case. The DOS is given in units of number of states per formula unit and Rydberg.

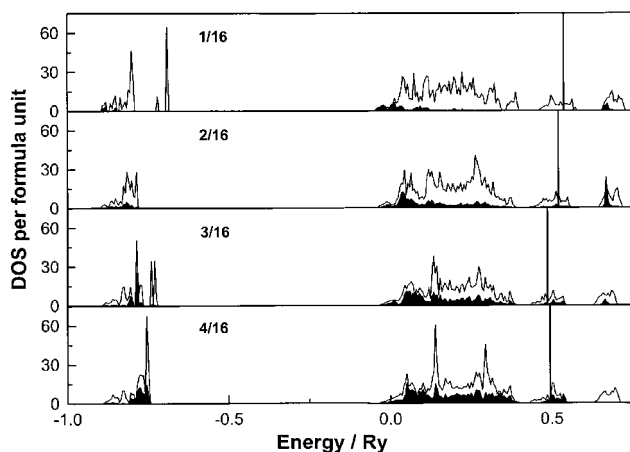


Fig. 9 The density of states (DOS) for the two types of lithium in $\text{Li}_{1+x}\text{Mn}_{2-x}\text{O}_4$ for the 16c case. The DOS is given in units of number of states per formula unit and Rydberg. The black areas are the DOS for the "extra" lithium at 16d positions; the white areas are for the lithium at 8a positions.

product.^{12,13} This can, in turn, explain differences obtained in the refined structures from different synthesis processes.

The intercalation potential

The open-circuit voltage (OCV) for the intercalation reaction described above is summarised in Fig. 11 using the assumption that only tetrahedrally coordinated Li can be cycled.¹⁴ As

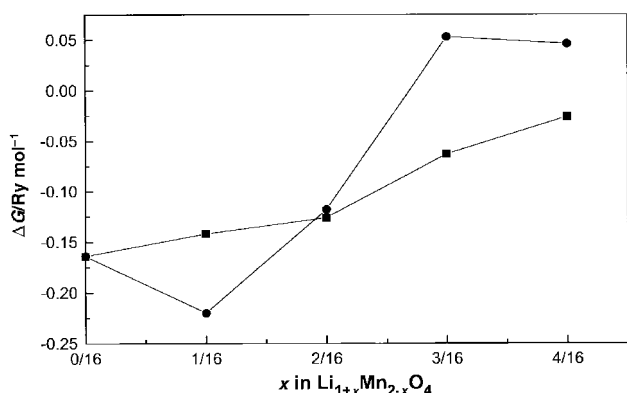


Fig. 10 ΔG for the reaction $\text{Li}_{1+x}\text{Mn}_{2-x}\text{O}_4 \rightarrow \text{Li} + \text{Li}_x\text{Mn}_{2-x}\text{O}_4$ as a function of x in $\text{Li}_{1+x}\text{Mn}_{2-x}\text{O}_4$ (● = 16d case, ■ = 16c case).

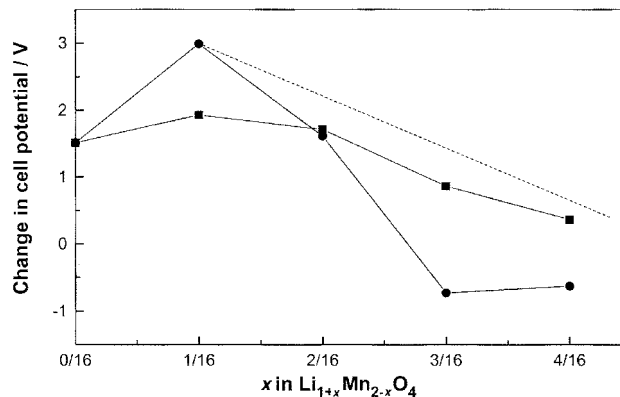


Fig. 11 The change in open-circuit voltage (OCV) as a function of x in $\text{Li}_{1+x}\text{Mn}_{2-x}\text{O}_4$. The dashed line indicates qualitatively the OCV for a phase with substitutions at both 16c and 16d positions (● = 16d case, ■ = 16c case).

mentioned previously, a substitution at the 16d position stabilises the structure for low degrees of substitution and increases the OCV. Above $x=1/16$ the actual OCV would be higher than that for the substitution of only one site type; the OCV for such a tentative mixture has been sketched in the figure. Substitutions higher than $x=1/16$ lead to a decrease in OCV and, above $x=2/16$, the OCV will be lower than that for the unsubstituted compound.

Conclusions

From LMTO-ASA band-structure calculations, it has been shown that, for low levels of lithium substitutions the 16d position is the most favourable for the "extra" lithium in $\text{Li}_{1+x}\text{Mn}_{2-x}\text{O}_4$. This result is in agreement with the work of Amundsen *et al.*²² At higher levels of substitution, a mixture of 16d and 16c positions substitution is most probable. This is in qualitative agreement with the results of Rietveld refinements of neutron powder diffraction data.^{10,11} However, the energy differences between the 16d and 16c positions are small and support refs. 12 and 13, which recognised that the chemical and electrochemical properties of manganate spinels are highly sensitive to the method of preparation. The intercalation potential increases to a maximum for small levels of substitution; higher levels of substitution lead to a decrease in the potential.

Acknowledgements

This work was supported by The Swedish Natural Science Research Council (NFR), The Swedish Board for Technical Development (NUTEK) and the EU (Joule III) Non-Nuclear Energy Sources Programme. All are hereby gratefully acknowledged.

References

- 1 M. M. Thackeray, P. J. Johnson, L. A. de Picciotto, P. G. Bruce and J. B. Goodenough, *Mater. Res. Bull.*, 1984, **19**, 179.
- 2 T. Ohzuku, M. Kitagawa and T. Hirai, *J. Electrochem. Soc.*, 1990, **137**, 769.
- 3 J. M. Tarascon, W. R. McKinnon, F. Coowar, T. N. Bowmer, G. Amatucci and D. Guyomard, *J. Electrochem. Soc.*, 1994, **141**, 1421.
- 4 R. J. Gummow, A. de Kock and M. M. Thackeray, *Solid State Ionics*, 1994, **69**, 59.
- 5 J. M. Tarascon, E. Wang, F. K. Shokoohi, W. R. McKinnon and S. Colson, *J. Electrochem. Soc.*, 1991, **138**, 2853.
- 6 R. Bittihn, R. Herr and D. Hoge, *J. Power Sources*, 1993, **43–44**, 223.
- 7 D. Song, H. Ikuta, T. Uchida and M. Wakihara, *Solid State Ionics*, 1999, **117**, 151.

- 8 J. C. Hunter, *J. Solid State Chem.*, 1981, **39**, 142.
- 9 H. Berg, J. O. Thomas, W. Liu and G. C. Farrington, *Solid State Ionics*, 1998, **112**, 165.
- 10 H. Berg, E. M. Kelder and J. O. Thomas, *J. Mater. Chem.*, 1999, **9**, 427.
- 11 H. Berg, Ö. Bergström, T. Gustafsson, E. M. Kelder and J. O. Thomas, *J. Power Sources*, 1997, **68**, 24.
- 12 M. M. Thackeray, A. de Kock, M. H. Rossouw, D. C. Liles, R. Bittihn and D. Hoge, *J. Electrochem. Soc.*, 1992, **139**, 363.
- 13 F. Le Cras, P. Strobel, M. Anne, D. Bloch, J. P. Soupart and J. C. Rousche, *Eur. J. Solid State Inorg. Chem.*, 1996, **33**, 67.
- 14 P. Endres, B. Fuchs, S. Kemmler-Sack, K. Brandt, G. Faust-Becker and H. W. Praas, *Solid State Ionics*, 1996, **89**, 221.
- 15 B. Ammundsen, J. Rozière and M. S. Islam, *J. Phys. Chem.*, 1997, **101**, 8156.
- 16 B. Ammundsen, M. S. Islam, D. J. Jones and J. Rozière, *Mol. Cryst. Liq. Cryst.*, 1998, **311**, 109.
- 17 K. Miura, A. Yamada and M. Tanaka, *Electrochim. Acta*, 1995, **41**, 249.
- 18 M. K. Aydinol, A. F. Kohan and G. Ceder, *J. Power Sources*, 1997, **68**, 664.
- 19 O. K. Andersen, *Phys. Rev. B*, 1975, **12**, 3060.
- 20 B. Nöläng, unpublished.
- 21 H. L. Skriver, *The LMTO Method, Springer Series in Solid State Science*, vol. 41, Springer, Berlin, 1984.
- 22 B. Ammundsen, D. J. Jones, J. Rozière, H. Berg, R. Tellgren and J. O. Thomas, *Chem. Mater.*, 1998, **10**, 1680.
- 23 A. A. von Zomeren, E. M. Kelder, J. Schoonman and E. R. H. van Eck, *The 1997 Joint Meeting of the Electrochemical Society and the International Society of Electrochemistry*, Meeting Abstract, vol. 97-2, p. 2507.